

Article

Pro-fluorogenic Reductase Substrate for Rapid, Selective, and Sensitive Visualization and Detection of Human Cancer Cells that Overexpress NQO1

William C Silvers, Bijeta Prasai, David H Burk, Matthew L Brown, and Robin Lindsey McCarley

J. Am. Chem. Soc., **Just Accepted Manuscript** • DOI: 10.1021/ja309346f • Publication Date (Web): 30 Nov 2012

Downloaded from <http://pubs.acs.org> on December 10, 2012

Just Accepted

“Just Accepted” manuscripts have been peer-reviewed and accepted for publication. They are posted online prior to technical editing, formatting for publication and author proofing. The American Chemical Society provides “Just Accepted” as a free service to the research community to expedite the dissemination of scientific material as soon as possible after acceptance. “Just Accepted” manuscripts appear in full in PDF format accompanied by an HTML abstract. “Just Accepted” manuscripts have been fully peer reviewed, but should not be considered the official version of record. They are accessible to all readers and citable by the Digital Object Identifier (DOI®). “Just Accepted” is an optional service offered to authors. Therefore, the “Just Accepted” Web site may not include all articles that will be published in the journal. After a manuscript is technically edited and formatted, it will be removed from the “Just Accepted” Web site and published as an ASAP article. Note that technical editing may introduce minor changes to the manuscript text and/or graphics which could affect content, and all legal disclaimers and ethical guidelines that apply to the journal pertain. ACS cannot be held responsible for errors or consequences arising from the use of information contained in these “Just Accepted” manuscripts.



Pro-fluorogenic Reductase Substrate for Rapid, Selective, and Sensitive Visualization and Detection of Human Cancer Cells that Overexpress NQO1

William C. Silvers,[†] Bijeta Prasai,[†] David H. Burk,[‡] Matthew L. Brown,[‡] and Robin L. McCarley^{†,*}

[†]Department of Chemistry, Louisiana State University, Baton Rouge, LA 70803-1804

[‡]Pennington Biomedical Research Center, Baton Rouge, LA 70808-4124

[‡]Department of Biological Sciences, Louisiana State University, Baton Rouge, LA 70803-1804

ABSTRACT: Achieving the vision of identifying and quantifying cancer-related events and targets for future personalized oncology is predicated on the existence of synthetically accessible and economically viable probe molecules fully able to report the presence of these events and targets in a rapid, and highly selective and sensitive fashion. Delineated here are the design and evaluation of a newly synthesized *turn-on probe* whose intense fluorescent reporter signature is revealed only through probe activation by a specific *intracellular* enzyme present in tumor cells of multiple origins. Quenching of molecular probe fluorescence is achieved through unique photo-induced electron transfer (PeT) between the naphthalimide dye reporter and a covalently attached, quinone-based enzyme substrate. Fluorescence of the reporter dye is turned on by rapid removal of the quinone *quencher*, an event that immediately occurs only after highly selective, two-electron reduction of the sterically and conformationally restricted quinone substrate by the cancer-associated human NAD(P)H:quinone oxidoreductase isozyme 1 (hNQO1). Successes of the approach include rapid differentiation of NQO1-expressing and non-expressing cancer cell lines via the unaided eye, flow cytometry, fluorescence imaging, and two-photon microscopy. The potential for use of the turn-on probe in longer-term cellular studies is indicated by its lack of influence on cell viability and its *in vitro* stability.

■ INTRODUCTION

Molecular probes whose fluorescent reporter signal is generated (turn-on probes) by enzyme activation¹ hold great potential for identification, enumeration, and study of living cancer cells—outcomes invaluable for accurate and early diagnoses and optimization of surgical and personalized chemotherapeutic treatments.^{2,3} In particular, the successful development of enzyme-activatable probes that can yield rapid, and highly sensitive and selective, reporting of species or events associated with cancer cells⁴⁻⁶ will allow for definition of diseased and healthy tissue borders during fluorescence-assisted surgical resection of cancerous tissues and collection of real-time information on tumor cell microenvironment or the pharmacodynamic effect of drugs on specific tumor cells.^{3,5-13} To date, live cancer cell detection with varying degrees of selectivity and sensitivity has been limited to routes employing extracellular or cell-surface protein recognition of a covalently attached component of the probe or reporter.^{3,12,14} However, successful identification of living cancer cells and their type differentiation can be achieved by targeting *endogenous, intracellular*, cancer-associated enzymes with hydrophobic *small-molecule* (<1000 Da), turn-on probes, an outcome not possible with large-molecule, recognition-based probes.

A potentially significant and unexplored route with turn-on probes for diagnostics is that in which selectivity and sensitivity of the target reporting process are controlled by *enzymatically stimulated removal of fluorescence quencher from the probe*. In particular, this route employs probes whose reporter fluorescence is quenched by photo-induced electron transfer (PeT)¹⁵ from a covalently attached enzyme substrate. Fluorescence ensues from the reporter upon removal of the quencher substrate by an endogenous, cytosolic, disease-associated enzyme found in diseased cells from a wide range of origins.

NAD(P)H:quinone oxidoreductase isozyme 1 (NQO1)¹⁶⁻¹⁹ is intimately involved with cancer, as it is a gatekeeper for the 20S proteasomal degradation of the p53, p73 α , and p33 tumor sup-

pressors¹⁶ and is present in a diverse group of human tumor cells (e.g., pancreas, colon, breast, lung, liver, stomach, kidney, head/neck, and ovaries) at levels 2- to 50-fold greater than in normal tissue.¹⁷ Furthermore, NQO1 content/activity in tumor cells is strongly affected by cell life cycle and therapeutic approaches.¹⁸⁻²⁰ Importantly, NQO1 is found in the cytosol and catalyzes the strict two-electron reduction of quinones to hydroquinones, making this flavoenzyme an ideal target for pro-drug therapies²¹ and pro-fluorophores.

Herein we report the design, properties, and NQO1-specific cellular activation of a first-generation, PeT-quenched fluorescence probe. The turn-on sensor probe readily penetrates the membrane of human cancer cells, because it is hydrophobic, small in molecular weight, and charge neutral. Upon rapid and preferential, two-electron reduction of the quinone quencher subunit of the turn-on probe, an intensely light-emissive reporter results from autonomous removal of the activated quinone subunit. Efficacious PeT quenching of fluorescence prior to subunit self cleavage is ensured by careful selection of the electronic properties of the naphthalimide reporter and quinone quencher. The resulting highly fluorescent, cationic reporter is retained by cells, and it exhibits a strong Stokes shift between its absorption and fluorescence emission maxima due to the push-pull internal charge transfer mechanism associated with the naphthalimide scaffold. Overall, these probe characteristics allow for rapid and enhanced signal-to-background imaging and detection of living cancer cells without the typical requirement of unactivated probe removal from the environment. In total, the pro-fluorogenic probe provides for real-time, highly sensitive and selective human tumor cell analysis and differentiation based on NQO1 content.

■ RESULTS AND DISCUSSION

Q₃NI Probe Fluorescence is Controlled by Photo-induced Electron Transfer (PeT) Quenching. We designed the Q₃NI probe to have the fluorescence signal of its naphthalimide reporter^{22,23} quenched via *oxidative* electron-transfer

(OeT) by the covalently attached quinone propionic acid motif, Figure 1A. It was posited that it would be possible to achieve this

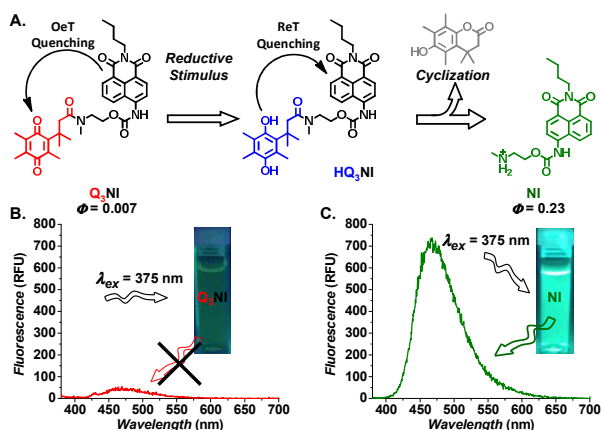


Figure 1. Schematic representation of the unique utilization of PeT quenching in the hNQO1 probe Q₃NI and the emission properties associated with Q₃NI probe and NI: (A) proposed quenching mechanisms for Q₃NI probe prior to and after chemical/hNQO1-catalyzed reduction, and subsequent production of the fluorescent NI reporter. Fluorescence spectra and optical images of cuvettes containing 2.0×10^{-6} M solutions of (B) Q₃NI probe and (C) NI reporter in pH 7.4, 0.1 M PBS that result from excitation at $\lambda_{ex} = 375$ nm (spectra) and $\lambda_{ex} = 365$ nm (images).

novel mechanism of reporter quenching by carefully tuning the electronic and optical properties of the quinone OeT quencher and the naphthalimide reporter NI, due to extant naphthalimide reporters that are quenched by *reductive* electron-transfer (ReT).²² The Rehm-Weller equation, Equation 1,

$$\Delta G_{PeT} = E_D - E_A - \Delta G_{00} - \frac{e^2}{\epsilon d} \quad (1)$$

was used to examine possible quinone propionic acid quenchers²⁴ and 1,8-naphthalimide reporters, as well as linkers between the OeT quencher and the NI reporter, so as to ensure that quenching is thermodynamically feasible and efficient.¹⁵ In this equation, E_D is the redox potential of the donor and E_A that of the acceptor, ΔG_{00} is the energy of the first excited singlet state of the reporter, and $e^2/\epsilon d$ is the Coulombic interaction energy of the ion pair, known to be 0.06 eV.¹⁵ The energy of the first excited singlet state of NI was measured to be 3.06 eV.¹⁵ From voltammetric measurements, E_D of NI was determined to be 1.74 V, and E_A for the quinone propionic acid group of Q₃NI was found to be -1.01 V (Figure S2). From these values, the energy change for this OeT process, ΔG_{PeT} , is calculated to be -0.37 eV, indicating that electron transfer from the excited dye to the electron-poor quinone is thermodynamically favorable. The quinone was attached to the naphthalimide via an *N*-methylethanolamine linker through a carbamate to the amine of the naphthalimide ring. This linker imparts three crucial properties on Q₃NI: the linker is sufficiently short to allow for a high probability of electron transfer, the electron-withdrawing carbamate yields a favorable ΔG_{PeT} , and the presence of the tertiary amide provides enhanced environmental stability.^{23,25} As a result, the fluorescence of Q₃NI in pH 7.4, 0.1 M PBS is effectively quenched in comparison to that of the free NI reporter, as noted by their spectra in Figure 1B and 1C and respective fluorescence quantum yields (Φ) of 0.007 and 0.23 obtained using quinine sulfate as standard.²⁶ The quantum yield for NI is superior or comparable to that of other dyes applied to cancer detection and localization, such as $\Phi = 0.0028$ for indocyanine green and $\Phi = 0.21$ for Cy5.5 dyes.^{13,27} The 33-fold fluo-

rescence enhancement for NI versus Q₃NI and very large Stokes shift of 116 nm ($\lambda_{max, abs} = 374$ nm, $\lambda_{max, em} = 490$ nm) bode well for use of Q₃NI as a multifunctional turn-on probe for sensing and imaging applications that utilize reductive stimuli capable of initiating removal of the reduced quinone group.²⁸⁻³¹

Fluorescence Dequenching of Q₃NI is Achieved by Reduction-initiated Removal of Quinone. We then wished to determine if it is possible to produce the NI reporter from the Q₃NI probe by the expected cyclizative cleavage reaction of the hydroquinone via the *gem*-dialkyl effect³² that occurs subsequent to two-electron reduction of the quinone.²⁸ Thus, the strong reducing agent sodium dithionite was added to aqueous solutions of Q₃NI. Under these conditions, it was found that NI is rapidly released as indicated by the increase in time-dependent fluorescence intensity (Figure 2) at 470 nm ($\lambda_{ex} = 370$ nm). To provide

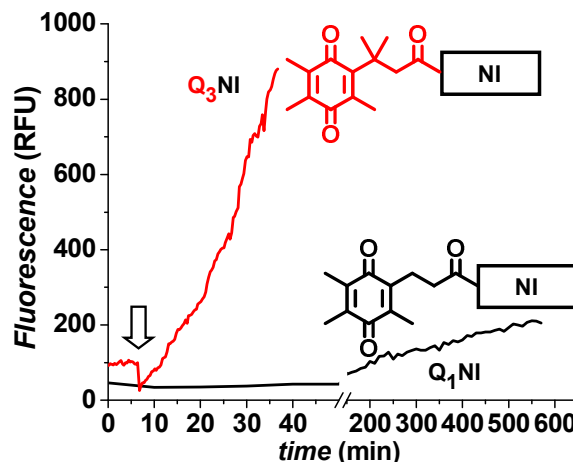


Figure 2. Comparing the dithionite-initiated formation of NI reporter from Q₃NI probe and Q₁NI. The fluorescence ($\lambda_{ex} = 370$ nm, $\lambda_{em} = 470$ nm) from 3-mL solutions of 1.0×10^{-5} M Q₃NI probe and Q₁NI in pH 7.4, 0.1 M PBS was monitored after their reduction by addition of 2.75 mg sodium dithionite (denoted by arrow).

proof positive that the increase in fluorescence for reduced Q₃NI results from cyclizative cleavage of the hydroquinone reduction product as the lactone, a second probe (Q₁NI) was synthesized such that the rate of lactone formation from its hydroquinone form is $>10^3$ times slower than in the case of reduced Q₃NI, due to the lack of the two methyl groups on the geminal carbon.²⁸ Dithionite reduction of the Q₁ group is known to be equally fast as the Q₃ group.²⁸ As seen in Figure 2, reduced Q₃NI exhibits exceedingly rapid NI reporter production in comparison to reduced Q₁NI; at 37 min (the maximum recorded for Q₃NI), the signal for reduced Q₃NI is 20-fold higher than that for Q₁NI. Although it could be argued the signal for reduced Q₃NI is attributable to the absence of photo-induced electron transfer quenching of the reporter by the hydroquinone of Q₃NI, a significantly favorable ΔG_{PeT} of -3.37 eV for the reductive quenching process of the NI reporter by the hydroquinone clearly supports its occurrence. That is, once the quinone is reduced to its hydroquinone (HQ₃NI, Figure 1A), quenching of reporter fluorescence occurs by reductive electron transfer (ReT), a common feature with naphthalimide dyes.²² Furthermore, we have isolated and identified the NI reporter from Q₃NI solutions treated with dithionite (Figure S-6). Thus, the rapid increase in fluorescence for reduced Q₃NI results from naphthalimide dequenching caused by reduction-initiated removal of the quinone propionic acid group by lactonization. Due to the unique quenching mechanism of the Q₃NI turn-on probe sensor, pronounced fluorescence signal enhancement upon revealing the NI reporter and its large Stokes shift, and the known resistance of

the quinone propionic acid trigger group to reduction by other biological species,³¹ we investigated **Q₃NI** as a sensor probe of human NAD(P)H:quinone oxidoreductase isozyme 1 (hNQO1) activity in real-time biological applications.

Q₃NI is Activated by hNQO1 at a High Rate. We determined if **Q₃NI** is a substrate capable of activation by hNQO1 to yield the **NI** reporter at a significant rate. To do so, we obtained the apparent kinetic parameters from Michaelis-Menten kinetic treatment³³ of the time-dependent **NI** reporter production, namely the Michaelis constant (K_m), maximum velocity (V_{max}), catalytic constant (k_{cat}), and substrate specificity (k_{cat}/K_m). The high rate of **NI** reporter production under in vitro conditions is readily apparent in the inset of Figure 3; after 5 min, a fluorescent signal has

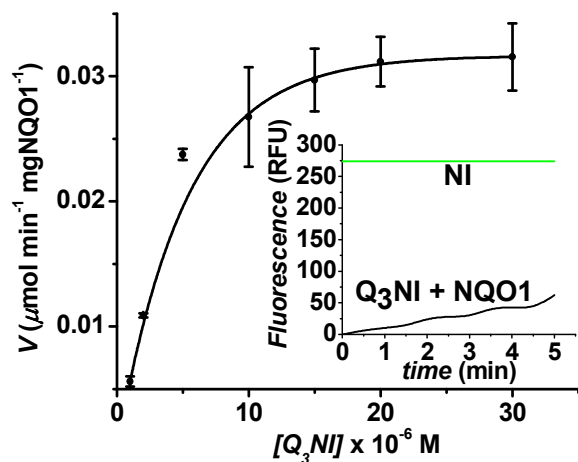


Figure 3. Kinetics plot of hNQO1 (2.0×10^{-5} g) toward **Q₃NI** Probe. Inset is an example of an assay observing fluorescent **NI** production from 1×10^{-6} M **Q₃NI**, relative to signal for complete **NI** formation (1×10^{-6} M). Values ($n = 3$) are the average \pm 1 standard deviation.

been attained that is 22% of the maximum achievable, yielding 2.2×10^{-7} M of released reporter. From the plot shown in Figure 3, we obtained $K_m = 3.86 \pm 0.79 \mu\text{M}$, $V_{max} = 0.037 \pm 0.002 \mu\text{mol min}^{-1} \text{mgNQO1}^{-1}$, $k_{cat} = 0.019 \pm 0.001 \text{ s}^{-1}$, and $k_{cat}/K_m = 4.94 \pm 0.33 \times 10^3 \text{ M}^{-1} \text{ s}^{-1}$. Due to the presence of the non-bulky ethanalamine linker and the need of only a single activation step to reveal reporter fluorescence, the kinetic constants are significantly higher than those of other NQO1 activatable fluorophores,^{31,34,35} thereby ensuring sufficient signal enhancement for fast detection of hNQO1 activity.

Cancer Cells can be Rapidly Visualized and Differentiated Based on hNQO1 Activation of **Q₃NI.** Our interest in the potential use of the **Q₃NI** probe in microfluidic-based cell sorting/isolation of circulating tumor cells³⁶ and fluorescence-guided resection of tumors³ led us to evaluate if the **Q₃NI** probe can be used to discriminate between cancer cells of different origins and hNQO1 content, with and without the aid of sophisticated instrumentation. The colorectal carcinoma cell line HT-29 and the non-small cell lung cancer (NSCLC) A549 cell line are known to possess significant hNQO1 activity, while the NSCLC H596 cell line has been reported to have undetectable hNQO1 activity.^{37,38} After a 10-min incubation period in a cell culture solution containing 2×10^{-5} M **Q₃NI**, it was possible to differentiate between the various substrate-cultured cells (4.84 cm²) using only a hand-held fluorescent lamp emitting at 365 nm and the unaided eye (Figure 4). Both HT-29 (3.69×10^6 total cells) and A549 (5.72×10^6 total cells) appeared fluorescent blue, while H596 (3.96×10^6 total cells) exhibited no apparent emission. The ability to visually determine the presence of hNQO1 in a small number of cells is due to the marked difference in fluorescence from

the unquenched **NI** reporter ($\Phi = 0.23$) and quenched **Q₃NI** probe

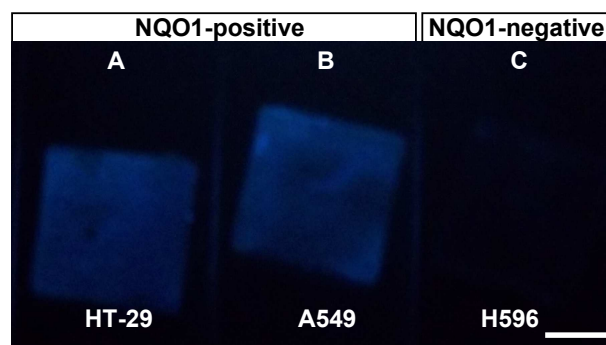


Figure 4. Visual differentiation of (A) HT-29, (B) A549, and (C) H596 cancer cells cultured on 2.2×2.2 cm glass substrates after 10-min incubation with 2×10^{-5} M **Q₃NI** probe. Images of cells were captured with a digital camera upon irradiation at $\lambda_{ex} = 365$ nm with a hand-held lamp. Scale bar represents 1 cm.

($\Phi = 0.007$) and the large Stokes shift of the **NI** reporter that results in fluorescence emission in the visible spectrum (400 nm to ~600 nm). These outcomes point to potential use of the **Q₃NI** probe sensor in the real-time, visible (without the aid of imaging equipment) and accurate determination of tumor/healthy tissue borders so as to allow for surgical resection of tumors with small foci.

Flow cytometry assays (Figure 5) were used to assess the applicability of the **Q₃NI** probe to rapidly detect and quantify tumor

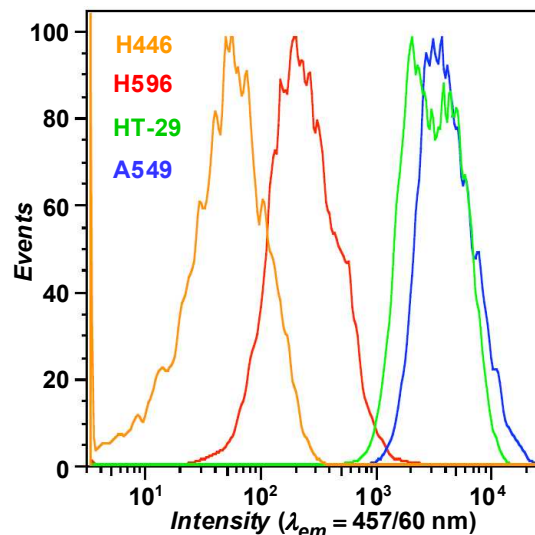


Figure 5. Flow cytometry assays of **Q₃NI** activation by hNQO1-positive (A549 and HT-29) and hNQO1-negative (H596 and H446) cancer cells. Assays were performed by counting 10,000 cells that had been exposed to 2.0×10^{-5} M **Q₃NI** probe for 10 min; $\lambda_{ex} = 405$ nm, $\lambda_{em} = 457/60$ nm.

cells containing hNQO1. The probe was incubated in a suspension of HT-29, A549, H596, and H446 (a small cell lung carcinoma known to be devoid of hNQO1 activity³⁷) cells for either 10 or 60 min, and a flow cytometer was used to measure the fluorescence ($\lambda_{ex} = 405$ nm, $\lambda_{em} = 457/60$ nm) in 10,000 individual cells. In Figure 5 are shown the histograms for each cancer cell line. It is clear that a high-intensity, unimodal distribution of signals is obtained for **Q₃NI** activation in each of the two hNQO1-positive cell lines (HT-29 and A549), while the negative cell lines H596

and H446 produced minimal fluorescence. It was also found that there was little change in the cell count or intensity of the histograms for a longer probe incubation time (60 min vs. 10 min, Figure S3), demonstrating the rapid and substantial activation of Q_3NI in A549 and HT-29 cells. Importantly, the sustained low fluorescence observed with the H446 cells (Figure S3) points to the intracellular stability of Q_3NI (lack of non-specific activation). Thus, it is indicated that Q_3NI is a highly sensitive and selective probe capable of being used to rapidly discern different types of tumor cells in fluidic streams.

Live and Fixed hNQO1-containing Cancer Cells can be Selectively Imaged via Q_3NI Activation. We desired to know if cancer cell types can be differentiated in conventional fluorescence microscopy images resulting from Q_3NI activation by hNQO1, and if it is possible to obtain images that allow collection of information regarding the fate of the released NI reporter. Furthermore, we wished to learn if the NI reporter can be successfully used in upconversion fluorescence (multi-photon) imaging of live cells.¹³ In agreement with flow cytometry data, wide-field imaging of fixed hNQO1-positive cells exposed to the Q_3NI probe for 10 min revealed significant probe uptake and activation that leads to intracellular NI fluorescence for the A549 and HT-29 cell lines; however, minimal signal was observed in the hNQO1-negative H596 cells (Figure S4). There was no indication of reporter in the nucleus, pointing to the lack of NQO1 there; this is in clear contrast to previous work using immunohistochemical staining of permeabilized, fixed cells.³⁹ The average cytosolic signal was 9 times higher in A549 cells versus NQO1-negative H596 cells, while it was 23 times higher in HT-29 cells compared to the NQO1-negative H596 cells. After incubating live HT-29 cells for 20 min with Q_3NI followed by exposure to acidic organelle-specific LysoTracker Red in the media in the imaging dish, it was found that the majority of the NI signal originated from the cytosolic region. Not surprisingly, accumulation of the basic (secondary amine $pK_a \sim 11$) NI occurred in acidic late endosomal and lysosomal vesicles (Figure S5), a beneficial outcome that leads to enhanced intracellular retention of NI. The higher signal-

to-background value achieved for activation of Q_3NI to NI reporter (9- to 23-fold) in target versus non-target cells, relative to that of other exogenously introduced sensor probes for whole tumor analysis (2.5- to 5-fold),⁴⁰⁻⁴² points to the potential of Q_3NI to provide highly selective tumor cell analyses with low limits of detection, even in the face of possible background fluorescence from hemoglobin and other species.¹ In addition, our results indicate that dye quantum yield is affected little, and there is no apparent efflux of NI reporter from cells during paraformaldehyde fixing, as noted by sustained fluorescence in fixed samples stored for 10 months in the laboratory ambient. Collectively, there is great potential for use of our probe/reporter system for *in vivo* quantitative analysis of excised tumor cells and long-term *in vivo* and *in vitro* imaging.

Multiphoton (MP) microscopy imaging of cells and tissues is more advantageous when compared to traditional fluorescence microscopy, because use of the characteristic long-wavelength photons offers higher fluorophore and cellular photostability that provides extended imaging duration, less background signal from out-of-focus excitation and scattering events, and deeper penetration depth. In addition, MP imaging is ideal for direct observation of targets in their physiological environment and *ex vivo* thick-specimen sampling where 2D and 3D maps can be generated.¹³ During incubation with complete growth medium containing 2.0×10^{-5} M Q_3NI , 2-photon microscopy revealed significant fluorescence signal from NI in living, hNQO1-positive HT-29 and A549 cells (Figure 6) and minimal signal in two living, hNQO1-negative cell lines, H596 and H446. The average fluorescence signal was determined to be 13-fold higher in A549 cells compared to H596 cells, and 3.66×10^4 -fold higher versus H446 cells. Similar results were obtained with the HT-29 cell line, with the cytosolic intensity being 15- and 4.51×10^4 -fold higher compared to H596 and H446 cells. As before, the signal appears somewhat heterogeneous throughout the cytosolic space of the HT-29 and A549 cells due to NI accumulation in acidic organelles. To ensure Q_3NI and NI had little effect on cell health, cells were incubated in a 2.0×10^{-5} M Q_3NI solution in complete

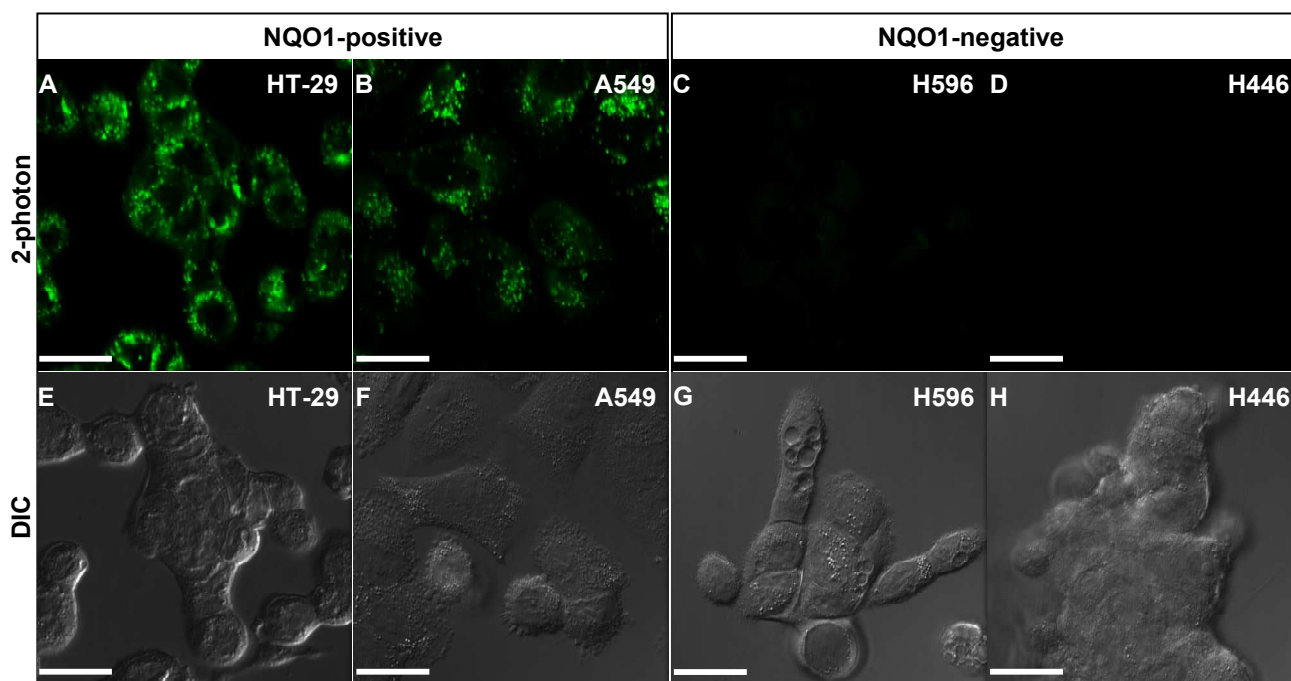


Figure 6. Two-photon confocal microscopy imaging of living HT-29 (A,E), A549 (B,F), H596 (C,G), and H446 (D,H) cells in the presence of 2.0×10^{-5} M Q_3NI probe. Fluorescence images of each cell line are on the top row with their respective differential interference contrast (DIC) image on the bottom row. Images were acquired at $\lambda_{ex} = 750$ nm (3% laser power) without any washing steps between Q_3NI probe addition and imaging. Scale bars represent 2.5×10^{-5} m.

growth medium for one hour and one day, and then cell viability was assessed with a trypan blue assay. After 1 h, cell viability for HT-29, A549, and H596 was 97.7%, 98.8%, and 100%, while it was 97.7%, 98.7%, and 98.4% after 24 h. Of particular importance is the real-time nature of the Q_3NI probe in imaging, as this system does not require the time-consuming wash steps characteristic of always-on reporters.^{1,4}

■ CONCLUDING REMARKS

In summary, we have presented the successful development and implementation of a quenched turn-on probe whose fluorescent reporter signal is selectively and quickly generated and maintained in human cancer cells upon activation by a cancer-associated-enzyme substrate that is subsequently removed from the probe to yield the free de-quenched reporter dye. Specifically, intracellular reduction of the quinone substrate by NAD(P)H:quinone oxidoreductase and successive self-removal of the reduced substrate from the reporter leads to elimination of the photo-induced electron-transfer quenching event, thereby yielding the naphthalimide reporter possessing a highly intense and Stokes-shifted emission. As a result, we have achieved rapid and highly selective/sensitive detection, differentiation, and enumeration of cancer cells in flowing streams and under traditional microscopy conditions without the use of recognition agents, an outcome that has in turn allowed for imaging of live cancer cells by multi-photon fluorescence microscopy. The latter outcome bodes well for in vivo and ex vivo thick-specimen imaging, where the efficacy of treatment protocols and the cellular impact of pharmaceutical targets can be evaluated for personalized oncology. Finally, control over the emission characteristics of the reporter dye²² coupled to our ability to visibly see, by the un-aided eye, relatively small numbers of cancer cells, reveals the potential of this new class of probes for application to fluorescence-guided surgical resection of cancerous tissues.

■ EXPERIMENTAL

Full details regarding materials, synthesis of compounds, and their characterization are described in the Supporting Information.

Cell Culture. HT-29 (human colorectal adenocarcinoma), A549 (human non-small cell lung cancer, NSCLC), H596 (human NSCLC), and H446 (human small-cell lung cancer) were all purchased from American Type Cell Culture. HT-29 cells were cultured in McCoy's 5A medium supplemented with 10% fetal bovine serum (FBS) and 100 IU/mL penicillin-streptomycin, A549 cells were cultured in F-12K medium with 10% FBS and 100 IU/mL penicillin-streptomycin, and H596/H446 were cultured in RPMI-1640 with 10% FBS and 100 IU/mL penicillin-streptomycin. Cells were incubated at 37 °C in a humidified incubator containing 5% wt/vol CO₂.

Flow Cytometry. To a 1-mL suspension of cells (1×10^6) in complete growth medium was added Q_3NI from a stock dimethyl-sulfoxide (DMSO) solution to give a final [Q_3NI] = 2×10^{-5} M and [DMSO] ~1%. After 10- or 60-min incubations at 37 °C, the cells were fixed with 30 mL of 4% paraformaldehyde in 0.1 M PBS for 1 h, followed by washing twice with 0.1 M PBS, and then resuspending in 1 mL PBS. Data acquisition was carried out on an iCyt Reflection flow cytometer using 405-nm excitation and a 457/60 nm emission filter; logarithmic amplification was used. Winlist software (Verity Software House, Topsham, ME) was used to count 10,000 cells per sample; FlowJo software was used to construct histograms.

Enzyme Kinetics. All fluorescence measurements ($\lambda_{ex} = 390$ nm, $\lambda_{em} = 470$ nm) were obtained at room temperature, with solutions composed of pH 7.4, 0.1 M PBS/0.1 M KCl/0.007% BSA. A stock solution of 1×10^{-4} M β -nicotinamide adenine dinucleotide, reduced disodium salt (NADH, Sigma-Aldrich), was made

with the PBS buffer; this NADH solution was subsequently used to prepare all other solutions so as to have a final concentration of 1×10^{-4} M β -NADH in each assay. Solutions consisting of 2×10^{-6} to 6×10^{-5} M Q_3NI were made using the NADH stock. A 1.33 μ g/mL stock solution of recombinant human NQO1 (Sigma-Aldrich) was prepared using the same buffer as above so as to give 2.0×10^{-5} g hNQO1 per assay. Each assay was performed in a quartz fluorescence cuvette containing 1.5 mL Q_3NI solution and initiated by the addition of 1.5 mL hNQO1 solution. Measurements were collected every 30 s for 5 min. Fluorescence units were converted to concentration by relating the signal increase to a fluorescence signal derived from a known concentration of NI . Plots of velocity versus Q_3NI concentration were used to obtain apparent K_m and V_{max} values from non-linear least squares analysis employing algorithms developed by Cleland for Michaelis-Menten kinetics.³³

Cell Viability. Cells were cultured in 5 mL of complete growth medium in a sterile tube. To the medium was added Q_3NI (from a 1.8×10^{-3} M stock solution) in DMSO, to give a 2.0×10^{-5} M Q_3NI solution, and the cells were incubated at 37 °C, 5% CO₂ for 1 h or 24 h, after which 1 mL of the cell suspension was removed and then 0.1 mL trypan blue was added. Cells were immediately counted using a hemocytometer and microscope.

Optical Differentiation. HT-29, A549, and H596 cells were cultured overnight on 2.2×2.2 cm glass cover slips. Old growth medium was removed and replaced with a 2.0×10^{-5} M Q_3NI solution in fresh growth medium. Cells were incubated at 37 °C with Q_3NI for 10 min and then rinsed with 0.1 M PBS. Cover slips of each cell line were immediately placed upside down on glass slides and visualized with a Kodak digital camera in conjunction with a Mineralight Model UVGL-25 lamp (365 nm, 0.16 amps, 60 Hz).

Confocal Colocalization. Confocal fluorescence images were acquired with a Leica TCS SP5 tandem scanning multiphoton laser scanning microscope using a 40x oil immersion objective lens (1.25 NA). Imaging of LysoTracker Red- and Q_3NI -exposed cells was accomplished using a sequential scanning method with $\lambda_{ex} = 405$ nm at 10% output and collecting emission between 417 and 467 nm (Q_3NI) or $\lambda_{ex} = 561$ nm at 10% output, and the emitted light was collected between 574 and 621 nm (LysoTracker Red). Differential interference contrast (DIC) images were obtained using a PMT detector and 633-nm light at 3% output as an illumination source. All images were collected at 37 °C using the Leica TCS SP5 in resonant scanning mode (16 KHz) at a zoom setting of 3.6. Images were line averaged 64 times. Cells were cultured overnight in black 35 x 10 mm, 22-mm well, glass-bottom dishes (Chemglass Life Sciences). Prior to imaging, the medium was removed and replaced with medium (containing no phenol red) and maintained at 37 °C. A concentrated solution of Q_3NI in DMSO was added directly to the dish to give a concentration of 2.0×10^{-5} M, with [DMSO] \leq 1%. Cells were incubated with Q_3NI for 20 min. Five min prior to imaging, LysoTracker Red-DND 99 in DMSO was added to give a concentration of 1×10^{-7} M.

In vitro 2-Photon Imaging. Two-photon confocal fluorescence images were acquired as above using a MaiTai two-photon laser tuned to 750 nm (3% laser power, modelocked Ti:sapphire laser; Tsunami Spectra Physics), and emission was collected using a short-pass 680-nm filter. DIC images were collected as above. Cells were imaged, with no washing or medium removal steps, after a 10-min incubation with Q_3NI . Image analysis was performed in ImageJ.

■ ASSOCIATED CONTENT

Supporting Information

Synthetic protocol and characterization data for Q_3NI , Q_1NI , and NI ; flow cytometry results; wide-field and confocal images of fixed cells exposed to Q_3NI . This material is available free of charge via the Internet at <http://pubs.acs.org>.

AUTHOR INFORMATION

Corresponding Author

tunnel@LSU.edu

Notes

The authors declare no competing financial interest.

ACKNOWLEDGMENTS

This material is based upon work supported by the US National Institutes of Health (5R21CA135585) and the US National Science Foundation under grant number CHE-0910845. This work utilized the facilities of the Cell Biology and Bioimaging Core that are supported in part by COBRE (NIH 8 P20-GM103528) and NORC (NIH 2P30-DK072476) center grants from the National Institutes of Health. We thank Drury Ingram and Marilyn Dietrich for help with flow cytometry experiments.

REFERENCES

- (1) Razgulín, A.; Ma, N.; Rao, J. *Chem. Soc. Rev.* **2011**, *40*, 4186-216.
- (2) Siegel, R.; Naishadham, D.; Jemal, A. *CA Cancer J Clin* **2012**, *62*, 10-29.
- (3) Nguyen, Q. T.; Olson, E. S.; Aguilera, T. A.; Jiang, T.; Scadeng, M.; Ellies, L. G.; Tsien, R. Y. *Proc. Natl. Acad. Sci. U.S.A.* **2010**, *107*, 4317-22.
- (4) Kobayashi, H.; Choyke, P. L. *Acc. Chem. Res.* **2010**, *44*, 83-90.
- (5) Luo, S.; Zhang, E.; Su, Y.; Cheng, T.; Shi, C. *Biomaterials* **2011**, *32*, 7127-38.
- (6) Shi, H.; He, X.; Wang, K.; Wu, X.; Ye, X.; Guo, Q.; Tan, W.; Qing, Z.; Yang, X.; Zhou, B. *Proc. Natl. Acad. Sci. U.S.A.* **2011**, *108*, 3900-5.
- (7) Blum, G.; von Degenfeld, G.; Merchant, M. J.; Blau, H. M.; Bogoy, M. *Nat Chem Biol* **2007**, *3*, 668-677.
- (8) Bremer, C.; Tung, C.-H.; Weissleder, R. *Nat Med* **2001**, *7*, 743-748.
- (9) Jaffer, F. A.; Kim, D. E.; Quinti, L.; Tung, C. H.; Aikawa, E.; Pande, A. N.; Kohler, R. H.; Shi, G. P.; Libby, P.; Weissleder, R. *Circulation* **2007**, *115*, 2292-8.
- (10) Simon, E. *Meas. Sci. Technol.* **2010**, *21*, 112002-112026.
- (11) Tung, C.-H. *Peptide Science* **2004**, *76*, 391-403.
- (12) Urano, Y.; Sakabe, M.; Kosaka, N.; Ogawa, M.; Mitsunaga, M.; Asanuma, D.; Kamiya, M.; Young, M. R.; Nagano, T.; Choyke, P. L.; Kobayashi, H. *Sci. Transl. Med.* **2011**, *3*, 110ra119.
- (13) van den Berg, N. S.; van Leeuwen, F. W.; van der Poel, H. G. *Current Opinion in Urology* **2012**, *22*, 109-20.
- (14) Ogawa, M.; Kosaka, N.; Choyke, P. L.; Kobayashi, H. *ACS Chem. Biol.* **2009**, *4*, 535-546.
- (15) Lakowicz, J. R. In *Principles of Fluorescence Spectroscopy*; Third ed.; Springer: 2006, p 331-351.
- (16) Dinkova-Kostova, A. T.; Talalay, P. *Arch. Biochem. Biophys.* **2010**, *501*, 116-23.
- (17) Danson, S.; Ward, T. H.; Butler, J.; Ranson, M. *Cancer Treat. Rev.* **2004**, *30*, 437-449.
- (18) Schlager, J. J.; Hoerl, B. J.; Riebow, J.; Scott, D. P.; Gasdaska, P.; Scott, R. E.; Powis, G. *Cancer Research* **1993**, *53*, 1338-1342.
- (19) Dong, G.-Z.; Youn, H.; Park, M.-T.; Oh, E.-T.; Park, K. H.; Song, C. W.; Kyung Choi, E.; Park, H. J. *International Journal of Hyperthermia* **2009**, *25*, 477-487.
- (20) Choi, E. K.; Terai, K.; Ji, I. M.; Kook, Y. H.; Park, K. H.; Oh, E. T.; Griffin, R. J.; Lim, B. U.; Kim, J. S.; Lee, D. S.; Boothman, D. A.; Loren, M.; Song, C. W.; Park, H. J. *Neoplasia* **2007**, *9*, 634-642.
- (21) Chen, Y.; Hu, L. *Medicinal Research Reviews* **2009**, *29*, 29-64.
- (22) Duke, R. M.; Veale, E. B.; Pfeffer, F. M.; Kruger, P. E.; Gunnlaugsson, T. *Chem. Soc. Rev.* **2010**, *39*, 3936-3953.
- (23) Qian, X.; Xiao, Y.; Xu, Y.; Guo, X.; Qian, J.; Zhu, W. *Chem. Commun.* **2010**, *46*, 6418-6436.
- (24) Mendoza, M. F.; Carrier, N. H.; Hettiarachchi, S. U.; McCarley, R. L. *Biochemistry* **2012**, *51*, 8014-8026.
- (25) Nicolaou, M. G.; Wolfe, J. L.; Schowen, R. L.; Borchardt, R. T. *The Journal of Organic Chemistry* **1996**, *61*, 6633-6638.
- (26) Fery-Forgues, S.; Lavabre, D. *J. Chem. Educ.* **1999**, *76*, 1260-1264.
- (27) Gioux, S.; Choi, H. S.; Frangioni, J. V. *Mol. Imaging* **2010**, *9*, 237-55.
- (28) Ong, W.; Yang, Y.; Cruciano, A. C.; McCarley, R. L. *J. Am. Chem. Soc.* **2008**, *130*, 14739-44.
- (29) Ong, W.; McCarley, R. L. *Macromolecules* **2006**, *39*, 7295-7301.
- (30) Ong, W.; McCarley, R. L. *Chem Commun (Camb)* **2005**, 4699-701.
- (31) Silvers, W. C.; Payne, A. S.; McCarley, R. L. *Chem. Commun.* **2011**, *47*, 11264-11266.
- (32) Milstien, S.; Cohen, L. A. *Proceedings of the National Academy of Sciences of the United States of America* **1970**, *67*, 1143-1147.
- (33) Cleland, W. W. *Methods Enzymol.* **1979**, *63*, 103-138.
- (34) Huang, S. T.; Lin, Y. L. *Org. Lett.* **2006**, *8*, 265-268.
- (35) Huang, S.-T.; Peng, Y.-X.; Wang, K.-L. *Biosensors & Bioelectronics* **2008**, *23*, 1793-1798.
- (36) Adams, A. A.; Okagbare, P. I.; Feng, J.; Hupert, M. L.; Patterson, D.; Gottert, J.; McCarley, R. L.; Nikitopoulos, D.; Murphy, M. C.; Soper, S. A. *J. Am. Chem. Soc.* **2008**, *130*, 8633-8641.
- (37) Beall, H. D.; Murphy, A. M.; Siegel, D.; Hargreaves, R. H.; Butler, J.; Ross, D. *Mol. Pharmacol.* **1995**, *48*, 499-504.
- (38) Smitskamp-Wilms, E.; Hendriks, H. R.; Peters, G. J. *General pharmacology* **1996**, *27*, 421-9.
- (39) Winski, S. L.; Koutalos, Y.; Bentley, D. L.; Ross, D. *Cancer Res* **2002**, *62*, 1420-4.
- (40) Andreev, O. A.; Dupuy, A. D.; Segala, M.; Sandugu, S.; Serra, D. A.; Chichester, C. O.; Engelman, D. M.; Reshetnyak, Y. K. *Proceedings of the National Academy of Sciences of the United States of America* **2007**, *104*, 7893-7898.
- (41) Shi, C. *Sci. Transl. Med.* **2012**, *4*, 1211e1.
- (42) Jiang, T.; Olson, E. S.; Nguyen, Q. T.; Roy, M.; Jennings, P. A.; Tsien, R. Y. *Proceedings of the National Academy of Sciences of the United States of America* **2004**, *101*, 17867-17872.

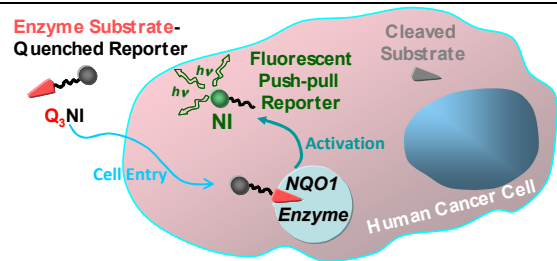


Table of Contents artwork